Hydrodynamics of Dense Fluidized Beds for Application in Concentrated Solar Energy Conversion

Benjamin Boissière, Hadrien Benoit, Renaud Ansart, Hervé Neau, Daniel Gauthier, Gilles Flamant, Mehrdji Hemati

Hydrodynamics of Dense Fluidized Beds for Application in Concentrated Solar Energy Conversion

Benjamin Boissière[14], Hadrien Benoit[2], Renaud Ansart[14], Hervé Neau[34], Daniel Gauthier[2], Gilles Flamant[2] Mehrdji Hémati[14]
[1] Université de Toulouse; INPT, UPS; LGC
4 Allée Emile Monso, BP 84234 31432 Toulouse Cedex 4, France,
[2] PROMES-CNRS; (UPR-CNRS 8521)
7, rue du Four Solaire, 66120 Font Romeu Odeillo, France,
[3] Université de Toulouse; INPT, UPS; IMFT
2 Allée du Professeur Camille Soula, F-31400 Toulouse, France,
[4] CNRS; Fédération de Recherche FERMAT; F-31400 Toulouse, France

Abstract

In the frame of the call for projects of the European Commission which aims to find alternative HTF in order to extend working temperature and to decrease environmental impact of standard Heat Transfer Fluid (HTF) used in concentrating solar power(CSP) plants, we proposed to use Dense Particle Suspensions -DPS- fluidized with air (approximately 50% of solid) in tubes as new HTF. DPS will enable operating temperature over 1 000 ˚C which corresponds to the sintering temperatures of the solid against 560 ˚C for the most efficient molten salts, thus increasing the plant efficiency and decreasing the cost per kWh produced, have no lower limitation of temperature and are riskless. A cold mockup of receiver using DPS has been built for the preliminary study of the concept. The operation of the mockup has shown the possibility to ensure a regular and adaptable upward flow of solid in the range 10 to $65\ \mathrm{kg \cdot h^{-1}}$ per tube. This paper compares the experimental results of the cold mockup running with the predictions of a multi-fluid approach 3D numerical code.

INTRODUCTION

In the field of high solar concentration industry, the reduction of the cost per kWh produced needs technical breakthroughs and innovations. Among the different solar concentration technologies: parabolic, fresnel, cylindrical-parabolic and central receiver system (CRS), the last one seems to be the most efficient (1). For central receiver, the increase in HTF operating temperature belongs to the most waited improvements because it will enable more efficient power cycles.

CRS mainly uses molten salts as HTF. Current molten salts have a melting point around 200 ˚C, making mandatory the use of auxiliary energy source during non-generation periods, and a maximal operating temperature of about 560 ˚C, which is too low to enable a supercritical cycle (2).

The proposed concept, concerns the HTF used in central receiver systems (3). To overcome the two previous drawbacks and to decrease the environmental impact of standard HTF, we suggest the use of dense gas-particle suspensions as an alternative heat recovery and storage fluid. These suspensions do not have lower temperature limit and the maximum operating temperature corresponds to the sintering temperature of the solid which is higher than 1000 ˚C. Moreover, as their volume composition is roughly 50% of solids and 50% of gas, their density and their volumetric heat capacity approximate that of a liquid.

The objective is to make these suspensions circulate into the solar absorber made of vertical pipes. The particles may then be used as an heat storage medium after being heated and stored in a storage vessel as it is currently done in CRS working with molten salts and as cannot be done by other fluids such as gas or steam.

In the frame of the "'CSP2" project, supported by the seventh Framework Program of the european commission (FP7), whose aim is the construction of a $150\ \mathrm{kW_{th}}$ solar pilot plant in the Odeillo solar furnace in France, a cold laboratory scaled mockup has been built at the Chemical Engineering Laboratory of Toulouse (LGC). This mockup must allow to understand and determine the operating conditions enabling stable and adjustable upward and downward solid flows (4). For this kind of fluid, the heat transfer efficiency is strongly linked to the particle agitation and the renewal rate at the wall, both unreachable with the available equipment. In order to access the local behavior of particles in an exchanger tube, we have undertaken 3D numerical simulations of this flow on a similar geometry with a multi-fluid approach code. In this paper, is presented the results of this work and the comparison with experiment.

EXPERIMENTAL STUDY

Experimental device: cold mockup

The mockup was designed to be tested under cold conditions. A detailed scheme is given Figure 1. It is a cold mockup of solar receiver made of two passes, one with vertical up-flow of solid and the other with downward flow of solid. Each pass is composed of two parallel tubes of $34\ \mathrm{mm}$ inside diameter made of transparent PVC. The bins are $400\ \mathrm{mm}$ height and have a $200\mathrm{x}400\ \mathrm{mm}$ base. The following only deals with the upward part of the solid flow.

The bottom bin is fluidized with $3\ \mathrm{Nm^3 \cdot h^{-1}}$ of air and is fed with solid by a hopper in the range $10\ \mathrm{kg \cdot h^{-1}}$ to $130\ \mathrm{kg \cdot h^{-1}}$. The freeboard pressurization of the bed by the regulation valve connected to a PID controller results in the rising of the solid in the tubes, until it reaches the top bin which is under atmospheric pressure.

The solid is silicon carbide mainly for its thermal properties, availability and low cost. The chosen particle size offers a good fluidization quality for very low air fluidization velocities.

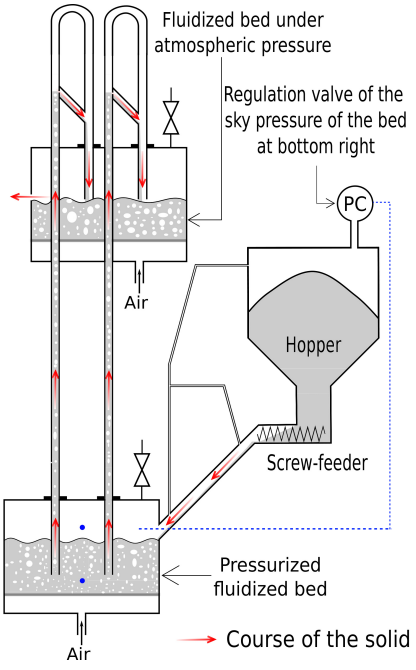

Figure 1: Overall design of solar receiver mockup.

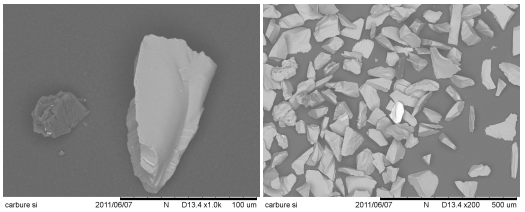

Figure 2: SEM photographs of SiC.

The minimum fluidizing and bubbling velocities and their corresponding solid volume fraction presented in Table 1 were determined experimentally.

Table 1: Properties of SiC.

Properties	ρ_p $(kg \cdot m^{-3})$	d_{32} (μm)	d_{50} (μm)	$Span$ $= \frac{d_{50}}{d_{90} - d_{10}}$	U_{mf} $(mm \cdot s^{-1})$	U_{mb} $(mm \cdot s^{-1})$	ε_{mf}	ε_{mb}
Values	3210	63.9	78.2	0.93	5.0	7.0	0.575	0.59

Metrology

The flow properties experimentally accessible are the static pressure of air and the gas flow rate going through each tube. Differential pressure controllers placed every $20\ \mathrm{cm}$ along the pipe allow to determine the average porosity of the suspension. Indeed, when the suspension is fluidized (air velocity higher than minimum fluidizing velocity), the pressure loss is equal to the solid weight divided by the tube section.

$$\Delta P = \frac{m_p \cdot g}{S} = \frac{(1-\alpha_g) \cdot \rho_p \cdot V \cdot g}{S} \Longrightarrow \alpha_g = 1 - \frac{\Delta P}{\rho_p \cdot g \cdot h} \tag{1}$$

The air flow rate going through each tube is determined with an helium tracking device. Helium is injected at a sufficient height of the tube to be sure to recover the totality at the top. The flow of air coming from the bin dilutes the helium. The air flow rate is given by the concentration of helium measured at the top of the tube through the Equation (2).

$$F_{air} = \left(\frac{1}{[He]} - 1 \right) \cdot F_{He} \tag{2}$$

The measurements were realized on a reference test case of $50\ \mathrm{kg \cdot h^{-1}}$ of solid per tube and a superficial air velocity of $15\ \mathrm{mm \cdot s^{-1}}$ for the fluidization of the bin.

A preliminary experimental study (4) has demonstrated , by determination of the fluidizing curve with decreasing air velocity, that the pressure loss sustained by air for the fluidization of this powder is about $130\ \mathrm{mbars \cdot m^{-1}}$. At the minimum fluidization state, the volume proportion of solid is about 0.43. This work has also shown that the same pressure profiles and the equal repartition of air between the tubes result in the same solid flow rate in each tube.

NUMERICAL SIMULATION

Mathematical model

Three dimensional numerical simulations are carried out using an Eulerian n-fluid modeling approach for poly-dispersed fluid-particle flows implemented in NEPTUNE_CFD software which is developed and implemented by IMFT (Institut de Mécanique des Fluides de Toulouse). This software is a multiphase flow code developed in the framework of the NEPTUNE project, financially supported by CEA (Commissariat à l'Énergie Atomique), EDF (Électricité de France), IRSN (Institut de Radioprotection et de Sûreté Nucéaire) and AREVA-NP. The multiphase eulerian approach is derived from a joint fluid-particle PDF equation allowing to derive the transport equations for the particle velocity's moment. In the proposed modeling approach, transport equations (mass, momentum and fluctuant kinetic energy) are solved for each phase and coupled through inter-phase transfer terms.The momentum transfer between the phases is modeled using the drag law of Wen & Yu limited by Ergun equation for the dense flows (5). The collisional particle stress tensor is derived in the frame of the kinetic theory of granular media (6). The turbulence modeling is achieved by the $k - \varepsilon$ model

extended to the multiphase flows (accounting for additional source terms due to the inter-phase interactions). For the dispersed phase, a coupled transport equation system is solved on particle fluctuating kinetic energy and fluid-particle fluctuating covariance ($q_p^2 - q_{fp}$). The effect of the particle-particle contact force in the very dense zone of the flow are taken into account in the particle stress tensor by the additional frictional stress tensor (7).

The mesh

The symmetry of the flow in each tube of the cold mockup allowed us to simplify the mesh geometry, thus limiting the calculation cost. The mesh includes one tube with the same dimensions as in the mockup and a bin with the same height.

The mesh (Figure 3) contains 1,650,000 hexahedra, based on O-grid technique with approximately $\Delta_r = 1.2\ \mathrm{mm}$ and $\Delta_z = 1.5\ \mathrm{mm}$. The chamber has a horizontal section area of $0.02\ \mathrm{m}^2$, a height of $40\ \mathrm{cm}$ and is equipped with a lateral solid entrance and a regulation valve at the top. The tube is plunged in the chamber. Its length is $2\ \mathrm{m}$ and it is set $10\ \mathrm{cm}$ above the bottom.

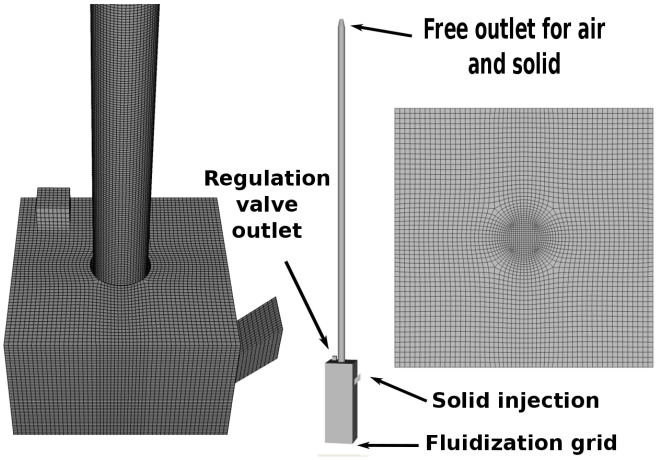

Figure 3: Mesh: the bin with one dipped tube.

Boundary conditions and phase properties

The geometry is composed of two inlets: the fluidization grid, which is a wall for the particles and where an air flow rate of $1.3\ \mathrm{kg \cdot h^{-1}}$ ($15\ \mathrm{mm.s^{-1}}$) is imposed and the lateral injection of solid in the bin with a solid flow rate of $50\ \mathrm{kg \cdot h^{-1}}$ at a $50\ \%$ porosity. There are also two outlets: the top of the tube is a free outlet for air and particles at atmospheric pressure, and an outlet placed at the top of the bin imitates the regulation valve. The pressure regulation valve is modeled as a pressure loss implemented on the cells of the valve conduct.

The pressure loss coefficient is defined as a function of the pressure in the chamber sky to imitate the behavior of the actual system, which uses a Proportional-Integral-Derivative (PID) controller.

The wall boundary conditions in the tube are defined as friction for the gas. For the particles, the influence of this boundary condition is studied at the section Boundary conditions and phase properties. The particles are taken monodisperse with a diameter of $64\ \mu\mathrm{m}$.

The calculations were run on 128 cores. The solid mass flow rate of the study case is $50\ \mathrm{kg.h^{-1}}$. The radial profiles presented are averaged over a section of the tube. The calculation of the average value begins when the transient regime is over. The steady state is reached when the weight of solid in the system becomes constant, in other words, when the solid flow rate exiting the tube is equal to the feeding solid flow rate.

Table 2: Influence of the wall boundary condition on the overall volume fraction of solid.

Wall boundary condition	Free-slip	No-slip	Friction	Experiment
Solid Volume Fraction	0.495	0.513	0.479	0.43

Table 3: Influence of the particle shape on the overall volume fraction of solid with free-slip condition.

Particle shape	Sphere	Strong non-sphericity	Experiment
Solid Volume Fraction	0.495	0.476	0.43

THE PRELIMINARY STUDY

Effects of numerical parameters

Before running the simulation on the complete geometry, we studied the effect of different numerical parameters on a simplified column geometry of $50\ \mathrm{cm}$ high and $36\ \mathrm{mm}$ of inner diameter.

The study of the mesh refinement with a fixed number of 30 width cells allowed us to determine the optimal mesh size for convergence. By comparing various cells heights from 1 to $5\ \mathrm{mm}$, we determined that the cell height had to be $1.5\ \mathrm{mm}$. With bigger cells the bubbles are dissolved and the flow becomes homogeneous, and using smaller ones only increase the number of cells with no difference in the results. As observed by Agrawal (8), the unresolved structures have a strong effect on macroscopic behaviour.

Several particle wall boundary conditions were tested. According to comparisons with PEPT measurements in dense fluidized bed, Fede et al. (9) have shown that free-slip boundary condition over estimates the downward mean particles velocity near wall region and that no-slip conditions improve that velocity profile. The Table 2 presents the averaged volumetric fraction of solid determined with the pressure profile measured at the wall depending on the wall boundary condition imposed for particles. The friction condition represented by a Johnson and Jackson boundary conditions (10) gives the closest results to the experiment.

As observed on Figure 2, the SiC particles are strongly non-spherical and present many angular shapes. This non-sphericity is considered by the correction of the drag coefficient through the coefficients C_{Shape} and f_{Shape} as described by Loth (11). With the morphological analysis of the particles, the coefficient C_{Shape} and f_{Shape} have been estimated to 5.3 and 1.15 respectively. This corresponds to a strong non-sphericity of the particles. The results of the 3 cases tested reported Table 3, shows that the solid volumetric fraction obtained with the strongly non-spherical shape is the closest to the experimental results.

Influence of gas compressibility

In order to study the effect of gas compressibility, the solid front ascending velocity have been studied in the case of no supply of solid, with a totally closed pressure regulation valve, and for a fluidizing air velocity of the bin of $15\ \mathrm{mm \cdot s^{-1}}$. Table 4 summarizes the experimental and numerical results of solid front velocity ascension for the incompressible case ($\rho_{gas} = \text{cst}$) and the case said “compressible” (the gas density follows the ideal gas law).

Table 4: Parameters for numerical simulation for the simulation 1.

	Incompressible	Compressible	Experiment
Solid front velocity	$0.28\ \mathrm{m.s^{-1}}$	$0.13\ \mathrm{m.s^{-1}}$	$0.08\ \mathrm{m.s^{-1}}$

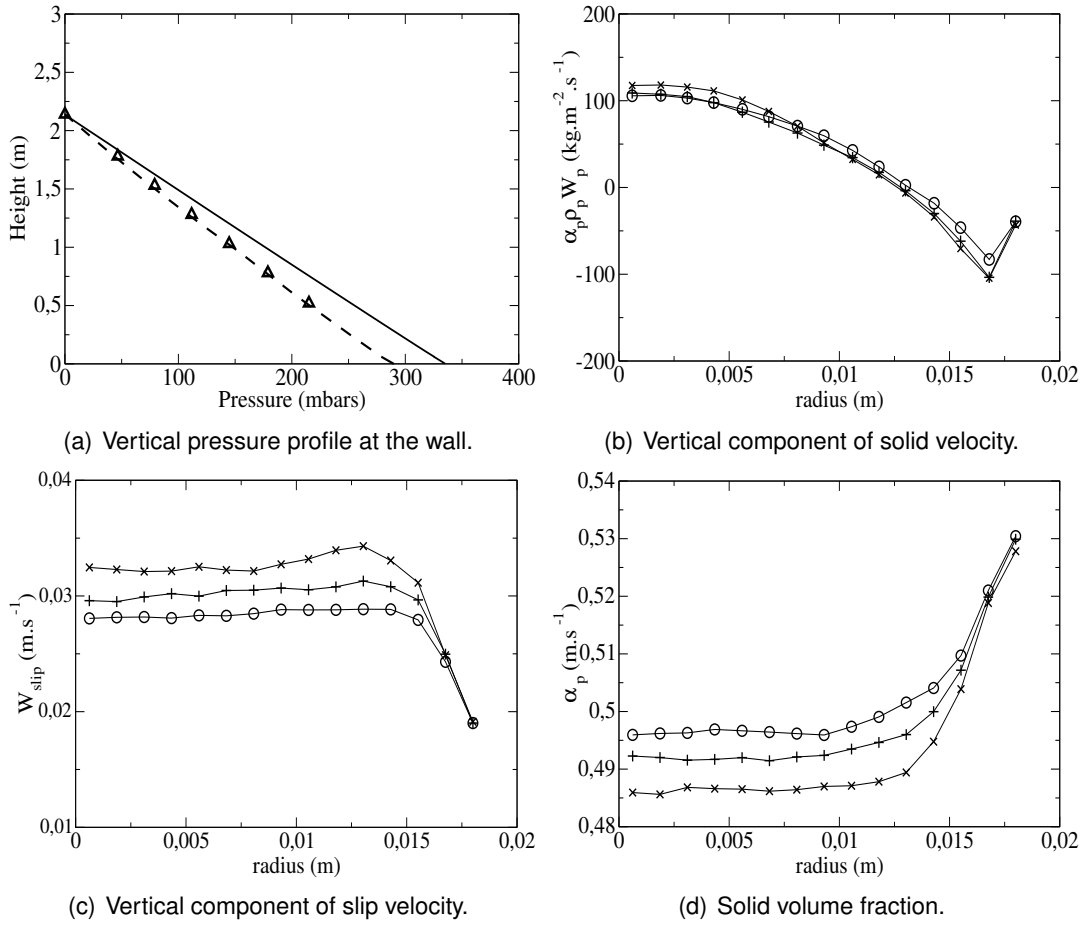

(a) Vertical pressure profile at the wall.

(b) Vertical component of solid velocity.

(c) Vertical component of slip velocity.

(d) Solid volume fraction.

Figure 4: (a) Vertical pressure profile at the wall. (– – –): Bubble-Emulsion prediction; (——): Multifluid approach prediction; (△): Experiment, (b)(c)(d) Radial profiles of vertical solid velocity, vertical slip velocity and solid volume fraction at different heights. (○): $\mathrm{z} = 0.5\ \mathrm{m}$; (+): $\mathrm{z} = 1.0\ \mathrm{m}$; (×): $\mathrm{z} = 1.5\ \mathrm{m}$.

This dynamic test shows the necessity to consider the gas compressibility in the si/-mulations. For the following of the study, we have considered the wall-particle boundary condition of Johnson and Jackson (10), a strong non-sphericity for the solid phase, and a gas density following the ideal gas law.

RESULTS

Comparison on pressure profile and gas flow rate

In this section, the radial profiles are presented by circumference and time averaging.

Figure 4(a) shows the gas pressure drop is linear along the tube for experimental measurements, 3D numerical simulation and for Bubble-Emulsion model prediction (4). These profiles are typical of pressure losses through fluidized beds. The numerical

prediction of the multi-fluid approach overestimates the pressure losses. This means that the volume fraction of solid is also overestimated. This difference between experiments and simulations can be attributed to the approximations that were done for the simulations: the particles were considered mono-disperse and spherical whereas the powder range of granular distribution goes from a few micrometers to more than a hundred and they have irregular, jagged shapes. The account of the poly-dipersed particles distribution needs to consider smaller particles which would require an even finer mesh. An alternative could be to use sub-grid model which take account of the effects on smaller scales (12) without decreasing the mesh dimensions and keep a reasonable CPU time. Meanwhile, the prediction of pressure profile of the 1D Bubble-Emulsion model modified to take account of the solid transport by bubble also presented 4(a) shows good agreement with experiment. This good agreement is mainly due to the hypothesis of an emulsion under the minimum fluidizing state.

The radial profiles of the vertical solid mass flux of the Figure 4(b) shows that there is a solid recirculation near the wall region. Indeed, the solid mass flux is positive at the center of the tube and negative near the wall. This recirculation of solid is a favorable flow property for the process efficiency because it enhances the renewal rate of particles at the wall and thus the thermal transfer.

Figure 4(c) shows that the solid is fluidized everywhere in the tube even near the wall region, because the slip velocity is higher than the interstitial minimum fluidizing velocity. The slip velocity increases with height of tube because. Indeed, the gas expansion with the decrease of pressure results in an increase of gas velocity.

Figure 4(d) shows that solid volume fraction is higher close to the wall. Solid volume fraction is lower at the base of the tube than at its top. It can be explain by the expansion of air resulting in higher slip velocities when rising in the tube.

CONCLUSION

The object of this paper was the experimental and numerical study of a new concept of solar receiver using DPS as new HTF, circulating in vertical narrow tubes.

The construction of a cold mockup has shown the possibility to have a constant and adaptable upward flow of solid, equally distributed between the tubes in parallel.

The analysis of the numerical parameters in a simple geometry has led to the following conclusions. The optimal cells for mesh are $1.2\ \mathrm{mm}$ wide and $1.5\ \mathrm{mm}$ high. A correction of the drag must be applied to take the particles shapes into account. The particles wall boundary conditions that best represents reality is a friction condition.

The simulation of the actual process was done step by step in a complex geometry. It was necessary to take the air density variation into account, which was done by the application of a perfect gas model. The process needs to be controlled, this is why a regulation was encoded. The analysis of the radial profile of particles vertical velocities shows that there is a solid recirculation in the tube. This recirculation observed qualitatively through the particle agitation will be an essential parameter for the thermal exchange.

Careful analysis of the results of these numerical simulations have to be led to determine the renewal rate of particles law near the wall. We will also study the effect of solid flow rate on these flow properties. In the frame of the european project

"CSP2", these numerical predictions will be compared to local measurements obtained by PEPT method (13).

ACKNOWLEDGMENTS

This work was developed in the frame of the CSP2 European project. Authors acknowledge the European Commission for co-funding the "CSP" Project (14) - Concentrated Solar Power in Particles - (FP7, Project N˚282 932). The simulations were carried out using the super-calculator Hyperion, to which we have access thanks to CALMIP (Calcul en Midi-Pyrénées), within the framework of the project P11032, and the authors are grateful to CALMIP for this.

REFERENCES

1. Ortega, J. I.; Burgaleta, J. I. and Téllez, F. M. "Central receiver system solar power plant using molten salt as heat transfer fluid", JSEE, 2008, Vol. 130, 024501.
2. Singer, C.; Buck, R.; Pitz-Paal, R. and Müller-Steinhagen, H. "Assessment of solar power tower driven ultrasupercritical steam cycles applying tubular central receivers with varied heat transfer media", JSEE, 2010, Vol. 132, 041010.
3. Hémati, M.; Flamant, G. "Dispositif collecteur d'Énergie solaire", Patent N˚10 58565, Oct. 2010.
4. Boissiere, B.; Ansart, R.; Gauthier, D.; Flamant, G.; Hémati, M. "Étude hydrodynamique d'un nouveau concept de récepteur solaire à suspension dense de particules.", Congrès Science et Technologies des Poudres, ENSIACET, Toulouse, 2012.
5. Gobin, A.; Neau, H.; Simonin, O.; Llinas, J. R.; Reiling, V. and Sélo, J. L. "Fluid dynamic numerical simulations of a gas phase polymerization reactor", Int. J. for Num. Methods in Fluids, 2003, Vol. 43, 1199-1220.
6. Boelle, A.; Balzer, G. and Simonin, O. (1995). "Second-order prediction of the prediction of the particle-phase stress tensor of inelastic spheres in simple shear dense suspensions", In Gas-Particle flows, Vol. 228, ASME FED. 9-18.
7. Srivastava, A. and Sundaresan, S. "Analysis of a frictional-kinetic model for gas-particle flow", Powder Technology, 2003, 129, 72-85
8. Agrawal, K.; Loezos, P. N., Syamlal, M. and Sundaresan, S. "The role of mesoscales structures in rapid gas-solid flows", J. of Fluid Mech., 2001, vol. 445, 151-185.
9. Fede, P.; Moula, G.; Ingram, T. and Simonin, O. "3D numerical simulation and PEPT experimental investigation of pressurized gas-solid fluidized bed hydrodynamic", In Proceedings of ASME 2009 Fluids Engineering Division Summer Meeting, ASME.
10. Johnson, P. C.; Jackson, R. "Frictional-collisional constitutive relations for granular materials, with applications to plane shearing", J. ofFluid Mech., 1987, Vol. 176, 67-93.
11. Loth, E. "Drag of non-spherical solid particles of regular and non regular shape", Powder Technology, 2008, Vol. 182, 342-353.
12. Parmentier, J. F.; Simonin, O. and Delsart, O. "A functional subgrid drift model for filtered drag prediction in dense fluidized bed", AIChE, 2011, Vol. 58, 1084-1098.
13. Chan, C. W.; Seville, J.; Yang, Z. and Baeyens, J. "Particle motion in the CFB riser with special emphasis on PEPT-imaging of the bottom section", Powder Tech., 2009, Vol. 196, 318-325.
14. CSP2 website: http://www.csp2-project.eu/home.html